NOVEL ICE DETECTION METHODOLOGY AND SYSTEM FOR SAFER AND GREENER AVIATION

Nicolas Fezans [1], Christoph Deiler [2]

[1][2] DLR (German Aerospace Center), Institute of Flight Systems, Lilienthalplatz 7, Braunschweig, 38108, Germany
[1] Email: nicolas.fezans@dlr.de, [2] Email: christoph.deiler@dlr.de

A novel robust ice detection methodology for the early detection of icing related flight performance degradation is presented. Based on data of $75,689$ flights with modern commercial airliners, a maximum aircraft fleet's performance variation is estimated. The evaluation of results indicates that an expected influence of icing could be clearly separated. The developed methodology is energy based and fuses aircraft body and engine influences on flight performance, which allows to reliably calculated a deviation from an available reference. This difference in flight performance is consequently used to detect an aerodynamic degradation. The novel methodology provides large capabilities and shows a good detection reliability with no false alarm even within maneuvering flight, wind shear, turbulence and sideslip.

Nomenclature

Symbols

α	angle of attack	rad
β	angle of side slip	rad
$\delta_{\text{Detection}}$	distance	m
Δf	function	
δl	distance	m
η	elevator deflection	rad
Φ	bank angle	rad
ξ	aileron deflection	rad
ζ	rudder deflection	rad
C_D	drag coefficient	
C_{D0}	zero lift drag coefficient	
$(\Delta C_D)_{\text{crit}}$	drag coefficient threshold	
$\Delta C_{\widetilde{D}}$	equivalent drag coefficient	
C_L	lift coefficient	
$\dot{E}$	energy change, power	W
g	gravitational acceleration	m/s^2
H	altitude	m
k_{ice}	icing severity factor	
Ma	Mach number	
m_{AC}	aircraft mass	kg
$\dot{m}_{\text{AC}}$	derivative of the aircraft mass	kg/s
n	load factor	m
N_1	engine fan speed	
$\mathcal{P}$	percentile/ quantile	
$\overline{q}$	dynamic pressure	Pa
S_{Wing}	wing surface area	m^2
t	time	s
u, v, w	translational velocities	m/s
V	velocity	m/s
x, y, z	body fixed coordinates	

Subscripts & Abbreviations

a	aerodynamic system
CAS	calibrated airspeed
comp	compensation term
corr	corrected
FDR	flight data recorder
IAS	indicated airspeed
IPS	ice protection system
k	kinematic system
opt	optimal
QAR	quick access recorder
ref	reference
TAS	true airspeed
tot	total
w	wind

1. INTRODUCTION

Icing can have a hazardous impact on the aircraft performance. In case of icing aircraft operational limitations might need to be adapted to remain in a safe flight envelope. During the last decades various accidents worldwide have shown the potential severity of icing-induced degradations as well as pilot's difficulties to recognize and cope with the corresponding changes in aircraft behavior [1–3]. The main degradation due to airframe (especially wing) icing manifests itself in a reduced stall angle of attack and increased drag. In the past, these effects of the icing phenomena have been investigated in various studies for different airfoils and icing cases (e.g. [4–6]) as well as for complete aircraft [7–10].

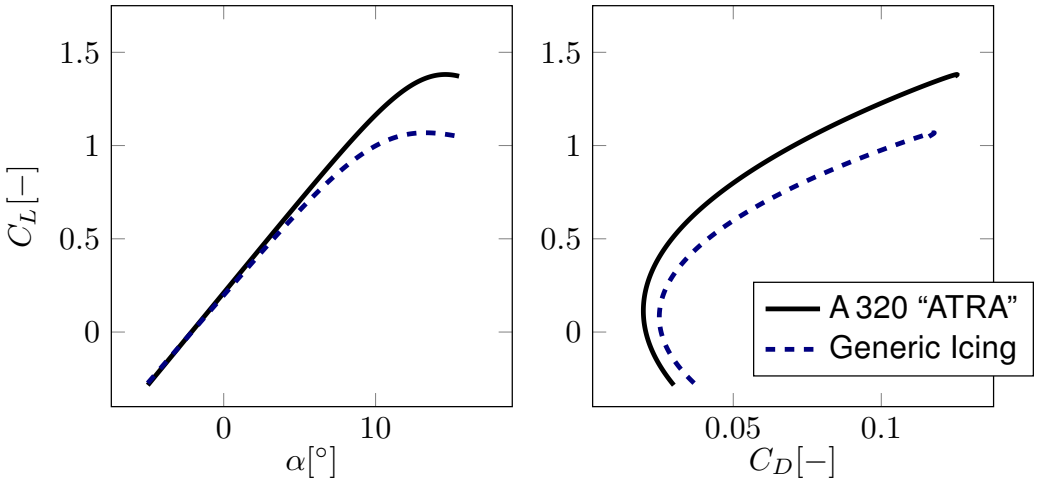

Figure 1. Comparison of A 320 “ATRA” lift and drag curve with and without generic icing influence

One major effect of aircraft ice accretion is a significant drag increase due to surface roughness changes, parasitic influence of ice protuberances, and local flow separation. Another effect of icing is a change of the aircraft lift behavior, with nonlinearities in the lift curve starting at a lower angle of attack than on the clean profile/wing (e.g. earlier or more abrupt flow detachment with increasing angle of attack). Figure 1 illustrates the typical estimated icing-induced modification of the lift and drag curves on the example of the DLR A 320 ATRA (Advanced Technology Research Aircraft) research aircraft. The generic icing curves shown in figure 1 are based on a light to moderate generic degradation with $25\,\%$ more zero lift drag, a $50\,\%$ higher polar curvature and $20\,\%$ reduced stall angle of attack.

Modern aircraft are equipped with anti-ice systems preventing ice accretion on critical parts or de-icing installations to remove ice shapes with a certain size. But these systems mainly are designed to fulfill existing certification requirements (Appendix C), which do not cover all icing types like for example supercooled large droplets (SLD) icing (nowadays covered by Appendix O). This means, that for existing aircraft there is a remaining (yet relatively remote) risk of ice accretion. Furthermore, all different existing ice protection systems (IPS) require an additional significant amount of energy on board. In case of thermal protection systems usually bleed air is used, which causes a reduction of the engine effectiveness and an increased fuel consumption. A deliberate activation of the IPS is necessary for efficient flight operations, which raises the demand for a reliable information about the current degradation, safety risk and therefore need to activate the IPS. This information could be provided by the herein proposed detection method.

This paper presents a novel methodology and system for the on-board surveillance of aircraft performance and its use for ice detection purposes. By providing pilots with a warning at a very early stage of ice accretion, aircraft safety is significantly increased in icing conditions, which was already shown by Bragg et al. in [11]. At that very stage, anti-ice / de-ice can be applied as countermeasures and the region in which icing conditions are encountered could still be left safely. The system with the herein proposed detection methodology can provide crucial information to the pilots while only requiring the sensor information that is available on all modern airliners and business jets. The developed system relies on the change in flight performance (i.e. steady flight states) contrary to the many failed attempts (e.g [11–16]) based on the estimation of changes in the aircraft's dynamic behavior. The change / degradation in the flight performance is an indicator of ice accretion that is both robust and highly available: unlike the approaches based on the detection of changes in the aircraft dynamical behavior, it can be used also during steady flight conditions (most of an operating flight) and can detect icing effects significantly before approaching stall. Apart from the safety improvement provided by this detection method, a more targeted use of extremely energy-consuming devices such as anti-ice systems could possibly be enabled.

Section 2 presents a first feasibility study that was made based on the data recorded by TUIfly during their regular operations. A brief descriptions of detection methodology and system implementation are given in section 3. First results to proof the detection reliability on the example of the DLR A 320 ATRA are finally shown in section 4.

2. NOMINAL VARIATION OF FLIGHT PERFORMANCE WITHIN A FLEET

Within a fleet of a single aircraft type the flight performance characteristics of each individual aircraft slightly differs. Some of the factors causing the flight performance variations across airplanes from the same type are:

- production tolerances,
- aircraft skin repairs,
- aircraft skin contamination (e.g. dirt),
- engine aging causing reduced efficiency,
- or engine contamination (e.g. dirt).

In order to be able to detect icing through the detection of flight performance changes, the other factors (i.e. nonrelated to icing) must be significantly lower than degradations caused by icing. Besides, the methodology proposed hereafter (section 3) uses the standard aircraft sensors and the measurement error (calibration and noise) also introduces variations in the determination of the aircraft flight performance.

All in all, the aircraft flight performance can be seen as follows

FlightPerformance
$=$ nominal Aircraft Flight Performance
$+$ nominal Engine Influence
$+$ *Variation*,

and the "*Variation*" part gathers the effects mentioned previously and is here the part that need to be analyzed.

In order to determine the typical and worst flight performance variation encountered during regular airline operations (due to a real performance variation or sensor errors), data of $75,689$ flights with Boeing B 737-700 and B 737-800 aircraft operated by TUIfly are analyzed. The data of each flight was recorded with the quick access recorder (QAR), which receives the same signals as the flight data recorder (FDR), and downloaded by the airline post-flight. The data resolution is different for the individual signals and reaches from 8 Hz (e.g. accelerations) to $1/64$ Hz (e.g. gross weight). No information about the aircraft thrust was recorded in the data and no engine simulation model permitting the calculation of these values out of measured engine parameters was available. This posed some difficulties for the intended analysis due to the major role played by the engines in the aircraft performance. This problem could be overcome acceptably well thanks to the huge quantity of data available. This was done by a segmentation in relatively short time-slices of about 60 s duration during which the aircraft is flying in a quasi-steady state: stabilized flight path (possibly climbing or descending) and possibly turning. Data segments with very dynamical maneuvers (e.g. high roll rate or rapid variation of load factor) were ignored in this analysis. Later on the segments are categorized according to their average speed, altitude, fan speed and outside air temperature. Each category describes an engine operating point allowing the estimation of a linear model describing the engine influence on the flight performance.

Unfortunately the data used for this analysis were partly anonymized such that the correspondence between a particular airplane and a recorded flight data was not available. As a consequence, all available information of the fleet is used together to estimate a global engine influence for the B 737-700 and B 737-800 separately. However, for this analysis it is crucial to consider the data from all the aircraft of the same type since the aim is to compensate the missing engine data / information but not to adjust the performance for each individual aircraft. The unavailability of the correspondence information prevented the detection of outliers in the data, which for instance happen if one of the airplanes has a significantly better or worse performance than the others. Eventually, this process enabled to estimate the missing information on the engines, but a real engine model would probably have been significantly more precise.

The methodology used to derive the aircraft performance from the recorded data is based on the energy of the airplane of rather its time-derivative. The total energy of the aircraft is

$$E_{\mathrm{tot}} = \frac{1}{2} \cdot m_{\mathrm{AC}} \cdot V_{\mathrm{TAS}}^2 + m_{\mathrm{AC}} \cdot g \cdot H \qquad (1)$$

and the time-derivative of the energy $\dot{E}_{\mathrm{tot}}$ describes the aircraft's real power imbalance, i.e. whether the total energy level is increasing for instance due to an excess of engine thrust for the current flight situation. The derivation of an engine model out of all the data is made by searching the model structure and parameter values that minimizes the error between the model-based computed reference power imbalance $\dot{E}_{\mathrm{tot,ref(P)}}$ (with P being the parameters of the model) and the actual power imbalance $\dot{E}_{\mathrm{tot}}$. Due to the high complexity of engine thrust models, a set of parameter values was determined (and later used) separately for each category. For each category, the problem can be formulated as:

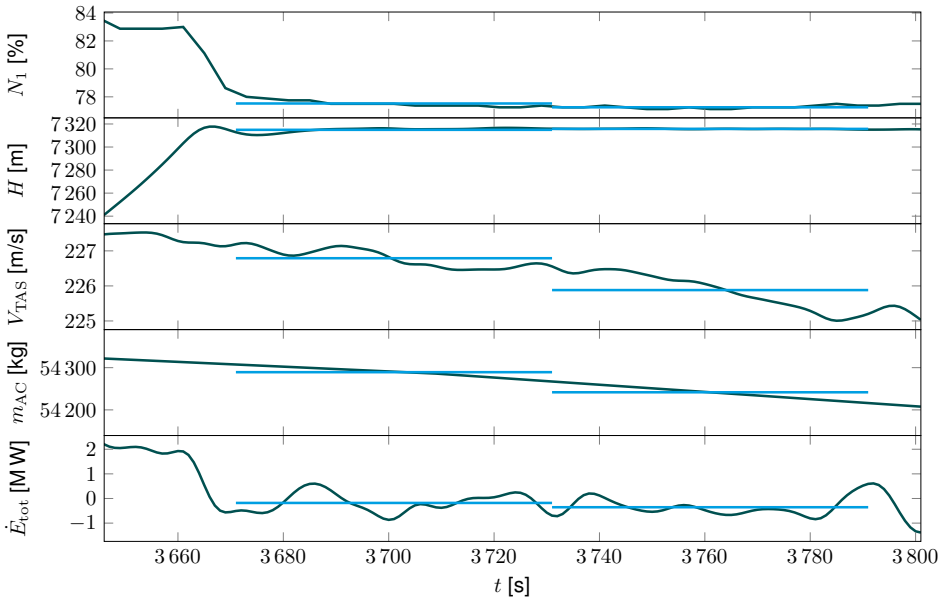

Figure 2. Example of automatically selected quasi steady segments in flight data

$$P_{\mathrm{opt}} = \mathrm{argmin}_P \left(\sum_{\mathrm{segments}} \left(\dot{E}_{\mathrm{tot,ref(P)}} - \dot{E}_{\mathrm{tot}} \right)^2 \right) \tag{2}$$

Later, in each category the vector of optimal parameter values P_{opt} is used and the corresponding power imbalance ($\dot{E}_{\mathrm{tot,ref(P_{opt})}}$) will be compared to the actual power imbalance $\dot{E}_{\mathrm{tot}}$.

In practice, before being able to find P_{opt} by solving the problem of equation (2) the data need to be preprocessed. This preprocessing includes the detection and cleanup of erroneous data (which can for instance happen at times when some onboard computers are being reset) as well as bringing the individual channels to the same constant sampling rate and time base. Then, the data are searched for steady engine and quasi-steady flight conditions for which several engine and flight parameters only slightly vary inside predefined boundaries. According to these conditions the flight data are segmented resulting in time slices of steady conditions with an individual length between $60\,\mathrm{s}$ and $120\,\mathrm{s}$. For each time slice mean values of altitude, speed / Mach number, temperature, gross weight, engine fan speed, fuel flow, and energy change are calculated and used for further evaluation. Using only mean values over data segments with steady flight conditions allows to reduce the data significantly although all necessary information is still available. An example of such segments is given in the time histories of several aircraft observation variables in figure 2. In the case shown in this figure, segments during cruise flight right after the aircraft climbed to $24,000\,\mathrm{ft}$ ($7,315\,\mathrm{m}$) are selected. With stabilized engine conditions the aircraft speed only contains small variations and the quasi steady flight assumption is valid.

With this method $202,797$ segments are extracted from the B 737-700 data and $5,161,814$ segments from the B 737-800 data. To use a regression technique for the estimation of the engine influence on the recorded aircraft flight performance, the data is categorized. It is possible to reliably estimate the engine model parameter values within a category only if this category contains enough segments. In the B 737-700 data base the 340 categories with the highest number of segments were selected and similarly in the B 737-800 data base the 750 categories with the highest number of segments were selected. The lowest number of segments in these categories were respectively 271 in the the B 737-700 case and 572 in the B 737-800 case. In both cases, an affine adjustment of the performance based on only three engine parameters (the fan speed N_1, the fuel flow $\dot{m}_{\mathrm{Fuel}}$, and the Mach number Ma) was found sufficient. Note that when applying an affine adjustment with only 3 linear terms (one per parameter) on data sets containing several hundreds of data points, there is no real risk of overfit.

Eventually, $\dot{E}_{\mathrm{tot,ref(P_{opt})}}$ (the reference power imbalance corrected from some of the unknowns affecting the engine thrust) can be written as:

$$\dot{E}_{\mathrm{tot,ref(P_{opt})}} = \dot{E}_{\mathrm{tot,ref}} + \Delta f \left(N_1, \dot{m}_{\mathrm{Fuel}}, Ma \right) \ , \tag{3}$$

with Δf being the optimal affine adjustment of the engine thrust model on the considered category.

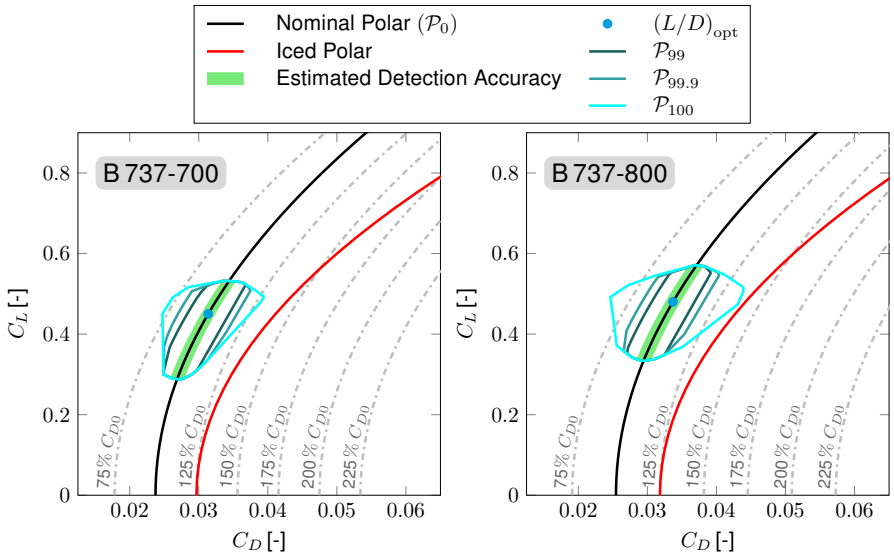

Figure 3. Obtained equivalent drag coefficient ($\mathcal{P}_{99}, \mathcal{P}_{99.9}$ & $\mathcal{P}_{100}$) within the two aircraft fleets

The remaining deviations between the expected power imbalance $\dot{E}_{\mathrm{tot,ref(P_{opt})}}$ and the actual power imbalance $\dot{E}_{\mathrm{tot}}$ (rate of change of the aircraft total energy) are the variations of the flight performance within the considered aircraft fleet. These variations are known to exist and need to be characterized in order to check the feasibility of a reliable icing detection system based on the monitoring of the aircraft performance. “Reliable” includes here (among others) the need to effectively detect the performance degradation due to icing while preventing false alarms.

While the chosen energy-based approach encompasses all aspects of the flight performance and especially the couplings between the involved physical parameters, the scaling of the power imbalance $\dot{E}_{\mathrm{tot,ref(P_{opt})}} - \dot{E}_{\mathrm{tot}}$ into a nondimensional equivalent drag coefficient variation $\Delta C_{\widetilde{D}}$ eases the physical interpretation (same order of magnitude for different speeds, current lift, or even aircraft type) and later on the definition of threshold values for the detection system (see section 3). This scaling is realized as follows:

$$\Delta C_{\widetilde{D}} = \frac{\dot{E}_{\mathrm{tot,ref(P_{opt})}} - \dot{E}_{\mathrm{tot}}}{V_{\mathrm{TAS}} \cdot \overline{q} \cdot S_{\mathrm{Wing}}} \tag{4}$$

The equivalent drag coefficient $\Delta C_{\widetilde{D}}$ computed using equation (4) describes the aircraft flight performance variation inside the fleet, mostly but not only resulting from variation of the aircraft aerodynamic performance (e.g. due to dirt, damages, or ice accretion). Other possible causes for this variation are sensor errors, unaccounted wind influences (e.g. downdrafts), and variations in the actual engine performance.

In order to represent the data (millions of data points) in an intelligible way, convex hulls (in the ($\Delta C_{\widetilde{D}}$,C_L)-plane) corresponding to several quantiles of the data were computed and represented graphically in figure 3 for the B 737-700 (left) and B 737-800 (right). On these individual figures:

- the black line represents the nominal drag polar of the aircraft,
- the dot-dashed gray lines are defined as by shifting the nominal drag polar by steps of $25\,\%\ C_{D0}$ and serve as grid in this figure,
- the red line represents an expected drag polar with moderate ice accretion comparable to figure 1,
- the green area represents schematically the accuracy that the authors expect to be able to reach with performance monitoring system shown later in section 3,
- the areas defined by the three cyan (with different brightness levels) polygon lines are the convex hulls of the selected data quantiles ($99\,\%$ $99.9\,\%$ and $100\,\%$).

There is several sources of errors affecting this analysis: a limited knowledge on the engine power characteristics of these two aircraft types, a low resolution (sampling-time and quantization) of the recorded data, a missing vertical wind information (which can hardly be recovered from the data available), and the fact that the B 737-800 data include aircraft equipped with different types of winglets. Note that these sources of errors are affecting this analysis of the recorded flight data but would not affect a detection system running aboard the aircraft.

After considering the knowledge gained from the data and the sensitivity of the results to the different sources of errors, an educated guess was made for the performance estimation uncertainty that can be reached in practice by an onboard system using the standard aircraft instrumentation (air data and inertial reference systems). The corresponding achievable precision is represented by the green areas in figure 3.

The results of this FDR / QAR data analysis support the initial guess that it is possible to monitor the aircraft performance of all aircraft from a complete fleet using the regular sensors and with a level of precision that permits to detect the performance degradation that is induced by the ice accretion at a very early stage (before this degradation of the performance reaches a critical level). The way the FDR / QAR data was processed in the analysis presented in this section was strongly tailored to a post-flight analysis. While some of the ideas used in the various processing steps can be reused for designing a real-time onboard detection system, numerous other refinements are needed for that application and will be shown in section 3 along with the description of the detection system.

3. DETECTION METHODOLOGY

In contrast to various published attempts to detect icing on changes of the dynamic aircraft behavior [11–17], the proposed method is focused on the flight performance changes. It is commonly known, that icing mainly affects the aircraft's drag (see figure 1), but none of the available methods is based on this effect. A major advantage of monitoring flight performance characteristics and not the aircraft's dynamic behavior is that no (additional) dynamic excitation is required. Such an excitation is not acceptable during normal operations as stated in [14], especially when flying with an icing degraded aircraft, which has a decreased maximum lift angle of attack.

The basic idea of the herein proposed detection method is to compare the current (possibly ice-influenced) aircraft flight performance characteristics with a known reference, as schematically represented in figure 4.

The flight performance can be formulated as a power imbalance (change of total energy) $\dot{E}_{\mathrm{tot}}$ in both cases (current state and reference), which allows to represent the changed aircraft characteristics in only one significant value and reduces the detection module complexity. Moreover, it combines the influences of aerodynamics and engines on the

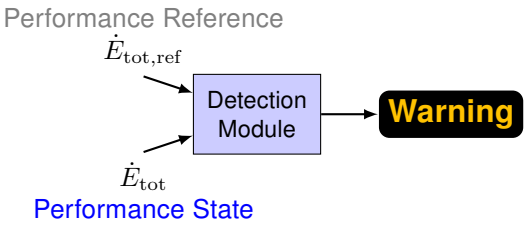

Figure 4. Basic principle of the detection method

aircraft performance. The power imbalance $\dot{E}_{\mathrm{tot}}$ is analytically derived through:

$$\begin{aligned}\dot{E}_{\mathrm{tot}} = \; & V_{\mathrm{TAS}} \cdot \dot{V}_{\mathrm{TAS}} \cdot m_{\mathrm{AC}} + \frac{1}{2} \cdot V_{\mathrm{TAS}}^2 \cdot \dot{m}_{\mathrm{AC}} \\ & + g \cdot \dot{H} \cdot m_{\mathrm{AC}} + g \cdot H \cdot \dot{m}_{\mathrm{AC}} \; ,\end{aligned} \tag{5}$$

with the altitude change $\dot{H}$ referenced to the surrounding air. The same scaling / conversion of this power imbalance into an equivalent drag coefficient variation as for the analysis of section 2 is used:

$$\Delta C_{\tilde{D}} \approx \frac{\dot{E}_{\mathrm{tot,ref}} - \dot{E}_{\mathrm{tot}}}{V_{\mathrm{TAS}} \cdot \overline{q} \cdot S_{\mathrm{Wing}}} \; . \tag{6}$$

This non-dimensional value is now well comparable to a predefined threshold and indicating an abnormal performance variation when exceeding the threshold value, independent from any trim condition. The fleet data evaluation in section 2 provides some concrete and objective data to define a suitable detection threshold, which guarantees a minimum expectable false detection rate with the standard sensor equipment and all possible influences on flight performance during normal airline operation. With the results shown in figure 3 a threshold value

$$(\Delta C_D)_{\mathrm{crit}} = 30\,\%\; C_{D0}$$

is conservatively defined, which suitably exceeds the detected performance variation. Generally speaking the choice of such a threshold is always trade-off between sensitivity and the probability of generating false alarms. For a given threshold value, the risk of generating false alarms might be reduced by improving the processing or by activating the system only under some particular conditions (e.g. for icing this could be based on some range of outside air temperature). The need to be prevent false alarms as much as possible, is that they could induce hazardous reactions (e.g. from the pilots) in otherwise totally safe situations. Even though this is not part of the scope of the present paper, it should be noticed that the risk of inducing hazardous reactions can be alleviated by a good human-machine interface design (making messages very understandable and precise to prevent confusion and misinterpretation) and by defin-

ing good procedures (i.e. basically directly providing the description of the right reaction).

3.1. REFERENCE MODEL FOR THE AIRCRAFT PERFORMANCE

The reference for the flight performance can be formulated in different ways, but in any case it must allow the computation of the aircraft energy evolution $\dot{E}_{\mathrm{tot,ref}}$ (power imbalance) for all relevant flight conditions. This power imbalance depends mainly on the atmospheric conditions, the aerodynamic properties of the aircraft, and the engine thrust. The aerodynamic properties of the (nominal) aircraft are usually very well known for the clean configuration, but a precise representation of the aerodynamic performance with spoiler / speedbrake deflections, high-lift, and / or gear extension might be more demanding. As a consequence, the system designer might choose to neglect some of the effects and as it will be seen later, there are easy ways to prevent that the detection system misbehave in the neglected situations.

One possible implementation of the reference model relies on a multi-dimensional table with values of $\dot{E}_{\mathrm{tot,ref}}$, which can be interpolated to obtain intermediate values between grid points. Each dimension represents one parameter describing the aircraft, atmosphere or engine state. In principle, the flight performance related energy change depends on altitude, airspeed, fan speed and lift as well as aircraft configuration. For each of these dimensions, there is usually several measurable parameters containing comparable information. For example altitude, static pressure, air density (among others) provide a similar information to the performance reference model, and the table could be built based on any of these variables. Similarly, several parameters could be used for airspeed (e.g. $V_{\mathrm{TAS}}, V_{\mathrm{IAS}}, V_{\mathrm{CAS}}, Ma$, etc.), engine state (e.g. engine pressure ratio, exhaust gas temperature, etc.) or lift force.

Note that the lift force is not always equal to the weight and the aerodynamic performance must be based on the lift force in order to be applicable in all conditions and especially during turns. The model quality of the tabular model depends on the used grid size, because smaller steps between the grid points allow to better cover nonlinearities in the characteristics. The table can be generated using various sources of information: model trim calculation of a dynamic aircraft model, flight data of corresponding flight conditions, etc. and must only be created once for a given combination of aircraft and engines.

3.2. CHALLENGES FOR RELIABLE ONBOARD FLIGHT PERFORMANCE ESTIMATION

During flight, current performance state $\dot{E}_{\mathrm{tot}}$ results from equation (5) using measurements of true airspeed V_{TAS} and altitude H as well as an information about the current aircraft gross weight m_{AC}. The mass change $\dot{m}_{\mathrm{AC}}$ of an civil aircraft is assumed to be directly correlated to the fuel flow $\dot{m}_{\mathrm{Fuel}}$ in all engines. The altitude time derivative $\dot{H}$ corresponds to the aircraft climb respectively sink rate and is normally also available in good quality from different sensors in flight.

The airspeed V_{TAS} is derived from several measurements and contains a combination of aircraft flight path velocity and wind speed (both to be understood as 3D vectors). Its derivative $\dot{V}_{\mathrm{TAS}}$ consequently also contains a component related to the change of both the altitude and inertial velocity vector as well as a component related to the change of wind vector. Only the first of these two components is relevant for the aircraft performance and the second component should be ignored / removed in order to prevent it from falsifying the performance estimate. The separation of the true airspeed time derivative in two parts

$$\dot{V}_{\mathrm{TAS}} = \dot{V}_{\mathrm{TAS},\dot{\vec{V}}_{\mathrm{k}}} + \dot{V}_{\mathrm{TAS},\dot{\vec{V}}_{\mathrm{w}}}, \tag{7}$$

can be obtained using a proper information about the wind encountered by the aircraft to calculate the airspeed change due to the inertial acceleration of the aircraft $\dot{V}_{\mathrm{TAS},\dot{\vec{V}}_{\mathrm{k}}}$ and due to a variation of the encountered wind $\dot{V}_{\mathrm{TAS},\dot{\vec{V}}_{\mathrm{w}}}$. The encountered wind can be estimated reliably for example by applying proper filter algorithms on measured air and ground speeds.

A variable wind corrected energy change $\dot{E}_{\mathrm{tot,corr}}$ results from equation (5) by using $\dot{V}_{\mathrm{TAS},\dot{\vec{V}}_{\mathrm{k}}}$ as an airspeed change:

$$\begin{aligned}\dot{E}_{\mathrm{tot,corr}} = \; & V_{\mathrm{TAS}} \cdot \dot{V}_{\mathrm{TAS},\dot{\vec{V}}_{\mathrm{k}}} \cdot m_{\mathrm{AC}} \\ & + \frac{1}{2} \cdot V_{\mathrm{TAS}}^2 \cdot \dot{m}_{\mathrm{AC}} \\ & + g \cdot \dot{H} \cdot m_{\mathrm{AC}} + g \cdot H \cdot \dot{m}_{\mathrm{AC}} \; .\end{aligned} \tag{8}$$

An mathematically equivalent way to correct the energy change for variable wind influences is to subtract the wind change influence from the energy change $\dot{E}_{\mathrm{tot}}$ calculated with equation (5):

$$\dot{E}_{\mathrm{tot,corr}} = \dot{E}_{\mathrm{tot}} - V_{\mathrm{TAS}} \cdot \dot{V}_{\mathrm{TAS},\dot{\vec{V}}_{\mathrm{w}}} \cdot m_{\mathrm{AC}} \; . \tag{9}$$

With the above correction, the energy change and the corresponding equivalent drag coefficient variation in a symmetric flight condition are available

and can be used for the abnormal flight performance detection. To further apply the methodology to asymmetric flight conditions, the additional estimated drag due to an angle of sideslip β must be compensated. This can be made by inserting a compensation term ($\Delta C_{D\beta,\mathrm{comp}}$) in the equation of the estimated equivalent drag coefficient variation introduced in equation (6) as follows:

$$\Delta C_{\widetilde{D}}(\beta) = \frac{\dot{E}_{\mathrm{tot,ref}} - \dot{E}_{\mathrm{tot,corr}}}{V_{\mathrm{TAS}} \cdot \overline{q} \cdot S_{\mathrm{Wing}}} - \Delta C_{D\beta,\mathrm{comp}} \,. \quad (10)$$

The compensation term $\Delta C_{D\beta,\mathrm{comp}}$ can be computed based on the lateral acceleration n_{y} and the sideslip angle β:

$$\Delta C_{D\beta,\mathrm{comp}} = -\frac{n_{\mathrm{y}} \cdot m_{\mathrm{AC}} \cdot g \cdot \sin\beta}{\overline{q} \cdot S_{\mathrm{Wing}}} \,, \quad (11)$$

and β could be directly measured if the aircraft is equipped with the appropriate sensors or estimated otherwise.

With the presence of ice contamination on the wing surface, the aircraft lift characteristics are altered. The shape of the ice accretion directly impacts the change in the aircraft's lift curve. With a significant deviation from the basic aircraft's lift curve a different angle of attack is necessary to obtain a similar lift from the wing for any given airspeed. In that case, the reference model as proposed in section 3.1 would give a wrong energy change for the current lift condition, assuming a lower angle of attack, and the additional drag could be underestimated. In order to cancel this effect an additional compensation term is proposed

$$\Delta C_{D\alpha,\mathrm{comp}} = (n_{\mathrm{z}} \cdot \sin\alpha + n_{\mathrm{x}} \cdot \cos\alpha) \cdot \frac{m_{\mathrm{AC}} \cdot g \cdot \sin\Delta\alpha}{\overline{q} \cdot S_{\mathrm{Wing}}} \,, \quad (12)$$

using the angle of attack difference $\Delta\alpha = \alpha - \alpha_{ref}$. The reference α_{ref} corresponds to the nominal angle of attack for this airspeed and lift / load factor, which can be computed based on the nominal aerodynamic model and / or stored in an additional multi-dimensional reference table. Note that this compensation significantly increases the complexity of the detection system and roughly doubles the resources needed (CPU, memory) while only compensating a relatively small error, as it can be observed on the results of section 4.1.

Rapid changes of wind (e.g. due to gust or turbulence) are too fast to be really relevant for the performance estimation: the best way to deal with them is certainly to apply a low-pass filter on the wind estimation and/or on $\Delta C_{\widetilde{D}}$ to cut off high frequency oscillations far larger than the possible performance change rates.

3.3. SYSTEM IMPLEMENTATION

A more detailed overview of the proposed method in figure 4 is given in figure 5. The incoming measurements are preprocessed to estimate the geodetic quasi steady wind field and suitably convert all data for the further steps. The multi-dimensional table (see section 3.1) used as reference model delivers the energy change $\dot{E}_{\mathrm{tot,ref}}$ expected for the current flight condition. The current true performance state $\dot{E}_{\mathrm{tot}}$ is for example evaluated according to equation (5) and corrected for wind, sideslip and lift change inside the detection module. This module finally triggers a warning flag if the additional calculated drag coefficient $\Delta C_{\widetilde{D}}$ exceeds some predefined threshold $(\Delta C_D)_{\mathrm{crit}}$.

In the implementation presented here and used for producing the results of section 4, the reference model does not account for any spoiler deflections, which significantly increase the aircraft's drag and decrease its lift. Within the normal flight operations, spoilers are only deflected during short period of time, but speedbrakes might be used during longer periods of time. Therefore it is found suitable to reduce the complexity of the reference model by not modeling asymmetrical spoiler deflections within the multi-dimensional tables. Including speedbrake drag in the model would enable the use of the detection system during the time they are extended, however it can be argued that the pilots would only be using the speedbrakes when being in a too high energy state (trying to descend and/or decelerate quickly) which are not the situations for which the proposed ice detection system is required. As a consequence, not covering speedbrake extension in the performance model can be an practicable option.

If not modeled spoiler / speedbrake-induced drag could be detected as a potentially icing-induced drag increase, which is prevented by defining and computing a confidence index based on its validity domain. In the case of spoiler / speedbrake extensions and also during aircraft configuration changes, this confidence index drops to zero and the detection algorithm is paused (in a frozen state) during that time. Note that this strategy is a design choice and by no means a limitation of the presented approach: the corrected handling of spoiler effects can be done by simply using a suitable reference model of the aircraft flight performance.

With all the presented corrections and a proper post-processing of $\Delta C_{\widetilde{D}}$, the herein proposed detection methodology gets robust against various influences and disturbances resulting in a minimum rate of false-positive detections. This behavior is essential for pilot's trust in the warning from a detections system.

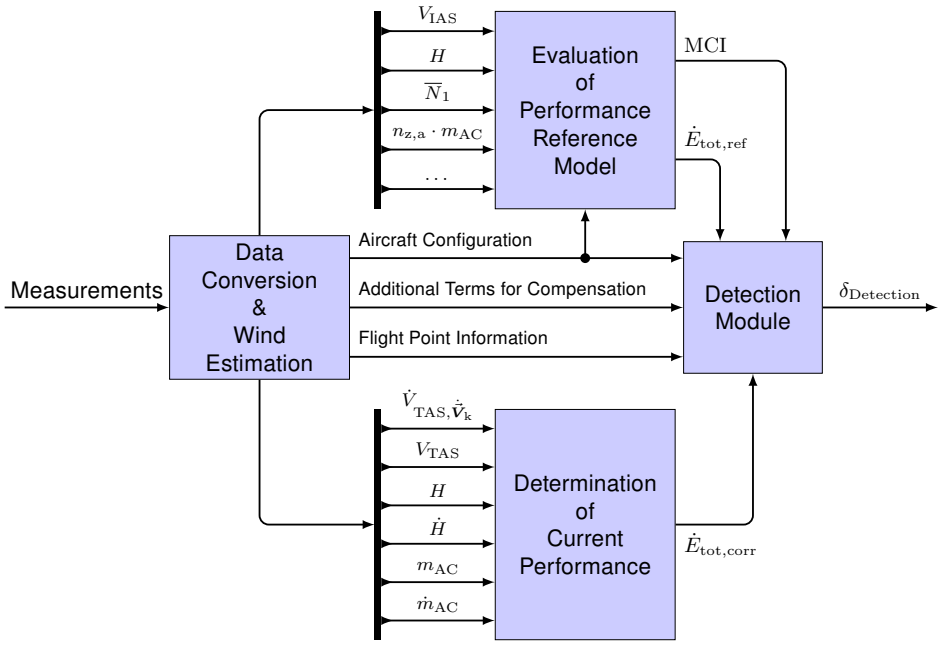

Figure 5. Possible implementation of the detection system

4. RESULTS

The novel energy-based icing detection method introduced in section 3 is applied to the DLR A 320 ATRA simulation model and tested hereafter with various scenarios. This model is a complete nonlinear flight dynamics model, including models for the sensor systems as well as advanced control laws and autopilot functions. This model has been extended to include a generic icing case as previously illustrated in figure 1. The icing severity parameter k_{ice} (similar to the definition in [11]) allows a continuous transition from the clean case (no ice $\Leftrightarrow$ $k_{\mathrm{ice}} = 0$) to the case shown in figure 1 ($k_{\mathrm{ice}} = 1$).

4.1. ICING ENCOUNTER

The purpose of the ice detection system is to detect early and reliably the performance degradation induced by the ice accretion. In order to illustrate the behavior of the system, the following simulation was performed. First, a slow ice accretion is simulated with k_{ice} going linearly from 0 to 1 in $500\,\mathrm{s}$. Then the iced state is kept for $140\,\mathrm{s}$ and finally the initial state (no ice) is restored by going from $k_{\mathrm{ice}} = 0$ also in $500\,\mathrm{s}$. This simulation was started with a trimmed horizontal flight at $11,000\,\mathrm{ft}$ and with and indicated airspeed of $220\,\mathrm{kt}$: this corresponds to a realistic holding condition in the neighborhood of an airport. The autopilot and autothrust hold this altitude and speed constant in spite of the disturbances caused by the ice accretion. Figure 6 shows the behavior of the main parameters. The icing severity parameter k_{ice} follows the aforementioned time evolution. The real power imbalance $\dot{E}_{\mathrm{tot,corr}}$ is always almost 0 since the aircraft continues to flight at constant speed and altitude, but the increased thrust level required for that leads the reference model to predict a significant power imbalance (large positive $\dot{E}_{\mathrm{tot,ref}}$). The difference between $\dot{E}_{\mathrm{tot,ref}}$ and $\dot{E}_{\mathrm{tot,corr}}$ leads in turn to a significant increase of the equivalent drag increase $\Delta C_{\widetilde{D}}$. By comparing $\Delta C_{\widetilde{D}}$ with the real drag increase C_D, it appears that they match pretty well. The drag increase is slightly underestimated, due to the phenomena describe earlier and that could have been compensated by using the formula of equation (12) but this compensation term was not used here in order to illustrate that this term might be neglected.

Apart from this slight underestimation, a slight phase-shift can be observed between C_D and $\Delta C_{\widetilde{D}}$: this results from a low-pass filter used on $\Delta C_{\widetilde{D}}$ to prevent false detection when sudden variations occurs, e.g. due to some gust or some non-physical effects (reset of an onboard computer during flight, entry of a corrected mass in the flight management system when possible). An additional safety against spurious changes of the detection flag / alarm can also be seen here: the status of the flag $\delta_{\mathrm{Detection}}$ only changes if the difference between $\Delta C_{\widetilde{D}}$ and $(\Delta C_D)_{\mathrm{crit}}$ has kept the same sign for a predefined time. Also a parameter that needs to be tuned based on the trade-off between sensitivity / reactivity of the system and false alarm rate.

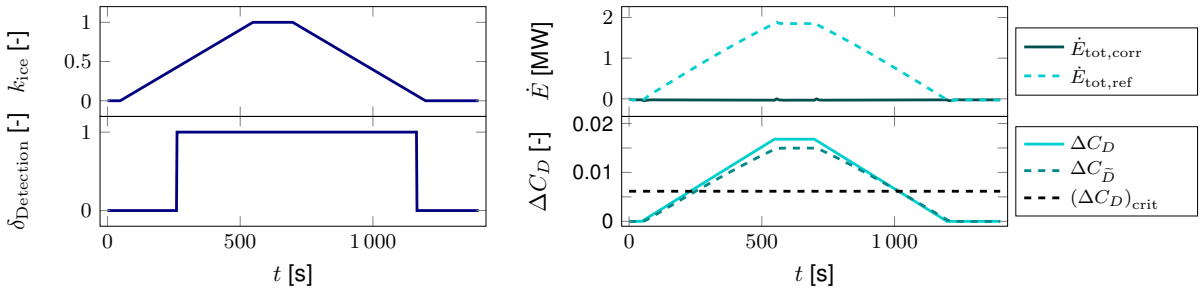

Figure 6. Behavior of the detection system during slow aerodynamic changes of the A 320 due to icing

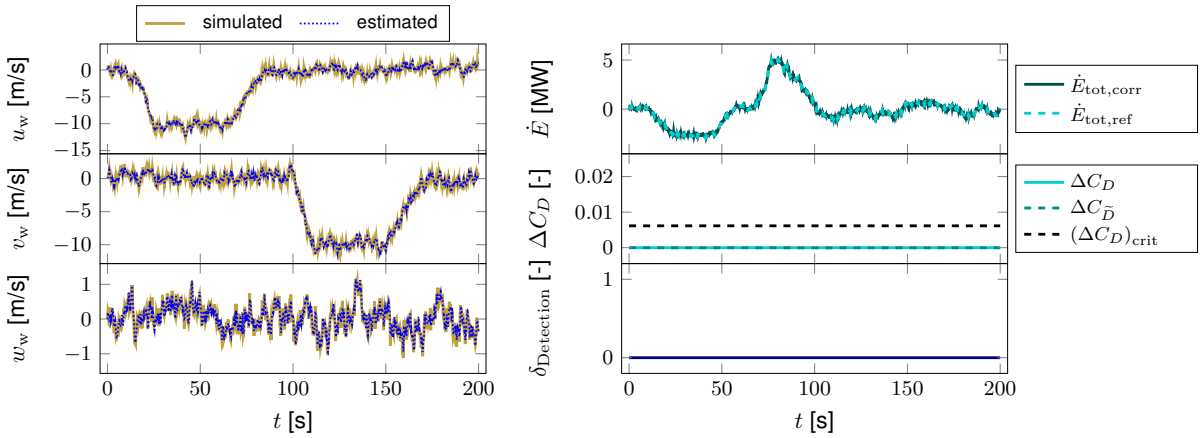

Figure 7. Behavior of the detection system in the presence of turbulence and wind shear

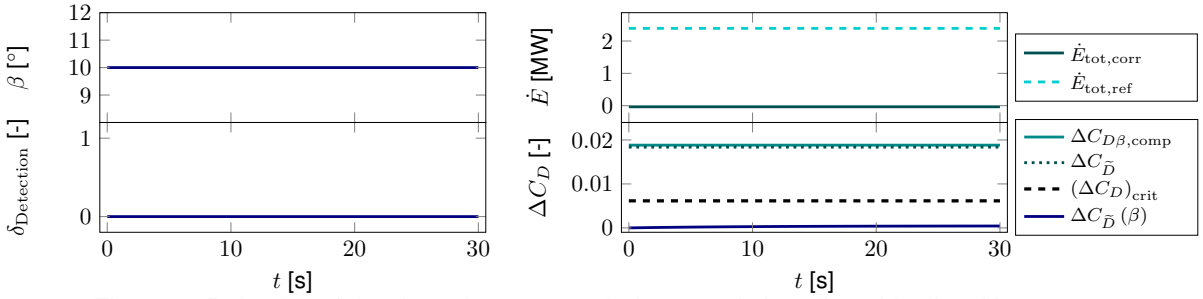

Figure 8. Behavior of the detection system during steady heading sideslip with $\beta = 10°$

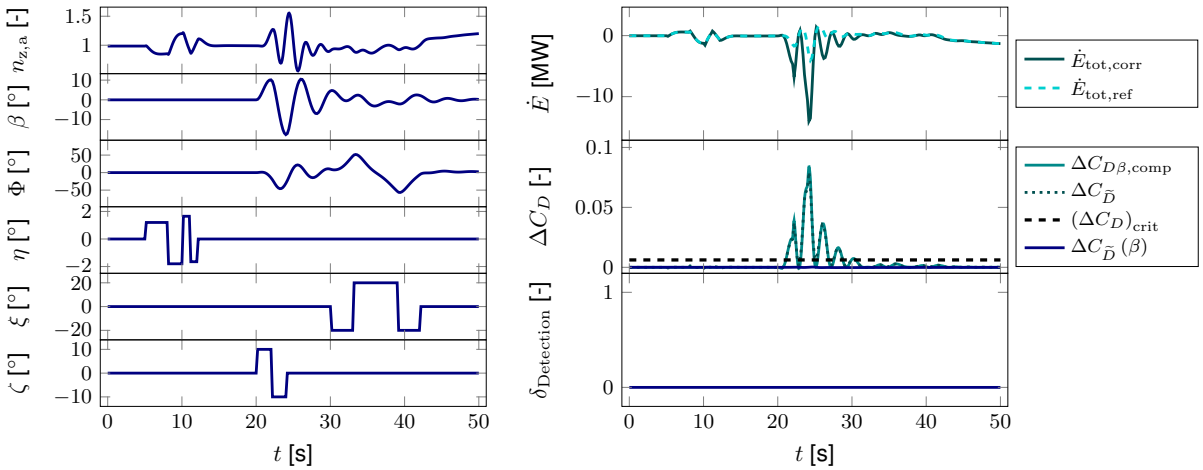

Figure 9. Behavior of the detection system during maneuvers (aircraft in “direct law”)

4.2. BEHAVIOR IN THE PRESENCE OF TURBULENCE AND WIND SHEAR

As it has been recognized in the derivation of the flight performance equations and explained in section 3.2, the temporal variation of the encountered wind poses some challenges for the design of a robust and reliable ice detection system on the basis of the aircraft performance. A scenario showing the behavior of the detection system when encountering wind changes in different frequency bands is shown in figure 7. The signals shown on the right side in this figures are defined exactly as in figure 6. On the left side, the simulated and estimated wind components (North-East-Down) are shown. The Kalman filter used for estimating the wind removes the high-frequency variations of the wind (which are not directly relevant for the flight performance) but tracks otherwise quite well the low and medium frequency changes of the wind vector. The encountered wind shear (change in wind velocity and orientation) is quite strong and the autopilot eventually rejects the corresponding change of energy but a significant transient response ($\dot{E}_{\mathrm{tot,corr}}$ and $\dot{E}_{\mathrm{tot,ref}}$ deviations from 0) occurred. However, the equivalent drag coefficient remains almost at zero during the whole simulation, which corresponds exactly to the desired behavior.

4.3. PRECISION OF THE SIDESLIP COMPENSATION

When using a reference performance model that only includes the performance during symmetrical flight (no sideslip), the additional drag that would be caused while slipping could be detected as an ice-induced performance degradation. This is prevented using the compensation term introduced in equations (10) - (11). In order to illustrate that a purely longitudinal performance model can indeed be precisely corrected by these terms to correctly handle sideslip conditions, a steady heading sideslip (with $\beta = 10°$) scenario was simulated (see figure 8). The sideslip compensation term is almost perfectly equal to the detected additional drag coefficient, such that the equivalent drag coefficient is almost zero.

4.4. CONTROL INPUTS

This last scenario illustrates the behavior of the developed system during active maneuvers on all three axes: pitch, roll, and yaw. In the pitching maneuvers, the handling of load factors different than one in the reference model lead to have $\dot{E}_{\mathrm{tot,corr}}$ and $\dot{E}_{\mathrm{tot,ref}}$ matching very well. The dynamical sideslip lead to three very significant nadirs in the $\dot{E}_{\mathrm{tot,corr}}$ curve: as expected the aircraft is losing energy (too much drag compared to the thrust) whereas the reference model does not predict it correctly since it contains no sideslip dependency. However, here again the sideslip drag coefficient compensation term follows the equivalent drag coefficient variation very well and prevent any false detection. During the final roll maneuver, which results in a large bank angle variation, the calculated and predicted energy change are matching again.

4.5. SUMMARY OF THE RESULTS

For all the cases on which the system was tested in simulation (including those not shown here), the system was able to detect the performance degradations that were introduced to the aircraft but not generate any false alarms when confronted with unsteady wind or maneuvers.

5. CONCLUSION

A novel ice detection method based on the monitoring of the energy state of the aircraft was presented. The validity and applicability of the approach is supported by two separated analysis. One the one hand it is supported by the analysis of the recorded data from a huge number of flights involving a fleet of aircraft from two aircraft types and during regular airline operations and on the other hand by simulations with various kinds of possible disturbances (wind, steady and dynamical maneuvers). The results are very promising and a patent covering all aspects of the presented system is pending.

ACKNOWLEDGEMENT

The authors want to specially thank TUIfly, in person Friedrich Lämmle and Moritz Horejschi, for providing the herein evaluated aircraft data and their colleague Dr. Fethi Abdelmoula, who converted the QAR flight records to processable data files.

References

[1] Green, Steven D.: *A Study of U. S. Inflight Icing Accidents and Incidents, 1978 to 2002*. Number AIAA 2006-82 in *44th AIAA Aerospace Sciences Meeting and Exhibit*, Reno, Nevada, USA, January 9th - 12th, 2006. American Institute of Aeronautics and Astronautics, Inc. (AIAA).

[2] N.N., *Final Report (BFU 5X011-0/98)*. Bundesstelle für Flugunfalluntersuchung, April, 2001, Braunschweig, DE.

[3] N.N., *Aircraft Accident Report (NTSB/AAR-96/01, DCA95MA001), Safety Board Report*. National Transportation Safety Board (NTSB), July 9th, 1996, Washington, DC, USA.

[4] Gray, Vernon H.: *Prediction of aerodynamic penalties caused by ice formations on various airfoils*. Technical Note D-2166, National Aeronautics and Space Administration (NASA), Washington, D.C., USA, February, 1964.

[5] N.N.: *Ice Accretion Simulation*. AGARD Advisory Report 344, Advisory Group for Aerospace Research & Development (AGARD) - Fluid Dynamics Panel Working Group 20, North Atlantic Treaty Organization (NATO), Neuilly-Sur-Seine, France, December, 1997.

[6] Broeren, Andy P.; Whalen, Edward A.; Busch, Greg T. and Bragg, Michael B.: *Aerodynamic Simulation of Runback Ice Accretion*. Journal of Aircraft, Vol. 47, No. 3, pp. 924–939, May-June, 2010.

[7] Ranuado, Richard J.; Batterson, J. G.; Reehorst, Andrew L.; Bond, T.H. and O'Mara, T. M.: *Determination Of Longitudinal Aerodynamic Derivatives Using Flight Data From An Icing Research Aircraft*. Number AIAA 89-0754 in *27th AIAA Aerospace Science Meeting*, Reno, Nevada, USA, January 9th - 12th, 1989. American Institute of Aeronautics and Astronautics, Inc. (AIAA).

[8] Ratvasky, Thomas P. and Ranuado, Richard J.: *Icing Effects on Aircraft Stability and Control Determined from Flight Data. Preliminary Results*. Number AIAA 93-0398 in *31st AIAA Aerospace Science Meeting and Exhibit*, Reno, Nevada, USA, January 11th - 14th, 1993. American Institute of Aeronautics and Astronautics, Inc. (AIAA).

[9] Lee, Sam; Barnhart, Billy P. and Ratvasky, Thomas P.: *Dynamic Wind-Tunnel Testing of a Sub-Scale Iced S-3B Viking*. Number AIAA 2010-7986 in *AIAA Atmospheric and Space Environments Conference*, Toronto, Ontario Canada, August 2th - 5th, 2010. American Institute of Aeronautics and Astronautics, Inc. (AIAA).

[10] Gingras, David R.: *Requirements and Modeling of In-flight Icing Effects for Flight Training*. Number AIAA 2013-5075 in *AIAA Modeling And Simulation Technologies (MST) Conference*, Boston, Massachusetts, USA, August 19th - 22th, 2013. American Institute of Aeronautics and Astronautics, Inc. (AIAA).

[11] Bragg, Michael B.; Başar, Tamer; Perkins, William R.; Selig, Michael S.; Voulgaris, Petros G.; Melody, James W. and Sater, Nadine B.: *Smart icing systems for aircraft icing safety*. 40th AIAA Aerospace Sciences Meeting and Exhibit, Reno, Nevada, USA, January 14th-17th, 2002. American Institute of Aeronautics and Astronautics, Inc. (AIAA).

[12] Bragg, Michael B.; Perkins, William R.; Sarter, Nadine B.; Başar, Tamer; Voulgaris, Petros G.; Gurbacki, Holly M.; Melody, James W. and McCray, Scott A.: *An Interdisciplinary Approach to Inflight Aircraft Icing Safety*. 36th AIAA Aerospace Sciences Meeting and Exhibit, Reno, Nevada, USA, January 12th - 15th, 1998. American Institute of Aeronautics and Astronautics, Inc. (AIAA).

[13] Myers, Thomas T.; Klyde, David H. and Magdaleno, Raymond E.: *The Dynamic Icing Detection System (DIDS)*. 38th AIAA Aerospace Science Meeting and Exhibit, Reno, Nevada, USA, January 10th - 13th, 1999. American Institute of Aeronautics and Astronautics, Inc. (AIAA).

[14] Melody, James W.; Başar, Tamer; Perkins, William R. and Voulgaris, Petros G.: *Parameter Identification for Inflight Detection and Characterization of Aircraft Icing*. Control Engineering Practice, Vol. 8, No. 9, pp. 985–1001, September, 2000.

[15] Aykan, Rahmi; Hajiyev, Chingiz and Caliskan, Fikret: *Aircraft Icing Detection, Identification and Reconfigurable Control Based On Kalman Filtering and Neural Networks*. AIAA Atmospheric Flight Mechanics Conference and Exhibit, San Francisco, California, USA, August 15th - 18th, 2005. American Institute of Aeronautics and Astronautics, Inc. (AIAA).

[16] Gingras, David R.; Barnhart, Billy P.; Ranuado, Richard J.; Ratvasky, Thomas P. and Morelli, Eugene A.: *Envelope Protection for In-Flight Ice Contamination*. 47th Aerospace Science Meeting, Orlando, Florida, USA, January 5th - 8th, 2009. American Institute of Aeronautics and Astronautics, Inc. (AIAA).

[17] Dong, Yiqun and Ai, Jianliang: *Research on inflight parameter identification and icing location detection of the aircraft*. Aerospace Science and Technology, Vol. 29, No. 1, pp. 305 – 312, August, 2013.